Asymptotic Convergence through Lyapunov-Based Switching in Extremum Seeking with Application to Photovoltaic Systems

Scott J. Moura and Yiyao A. Chang

***Abstract*—This paper presents a practical extension to extremum seeking control systems which guarantees asymptotic convergence through a Lyapunov-based switching scheme. In contrast, traditional extremum seeking methods enter a limit cycle around the optimal set-point, once identified. The proposed approach converges to the optimal set-point by exponentially decaying the sinusoidal perturbation signal once the system enters a neighborhood around the extremum. To analyze the performance characteristics of this method, we apply this algorithm to the maximum power point tracking (MPPT) problem in photovoltaic systems. Simulation results indicate that our approach is self-optimizing in the presence of varying environmental conditions and produces higher energy conversion efficiencies than traditional MPPT methods under typical operating scenarios.**

I. Introduction

Extremum seeking (ES) deals with the problem of regulating a system to an unknown optimal set-point. Since we assume the cost function that maps input to performance output is unknown, a periodic perturbation signal is typically used to probe the space. However, once the closed-loop system has identified the optimal set-point, most methods enter a limit cycle around this point as opposed to converging to it exactly. Hence, one of the main challenges with ES is guaranteeing asymptotic convergence to the optimal set-point – not in the average sense, but the exact sense. This paper investigates a novel Lyapunov-based switched extremum seeking (Lyap-ES) approach that guarantees asymptotic convergence to the optimal set-point. The proposed concept is demonstrated on a well-studied yet important problem: maximum power point tracking (MPPT) in photovoltaic (PV) systems.

Prior to the nonlinear and adaptive control theory developments in the 1970's and 1980's, extremum seeking was proposed as a method for identifying the minimum or maximum of an equilibrium map. Since then, researchers have extended extremum seeking to the general class of nonlinear dynamical plants (see e.g. [1], [2]) and applied the algorithm to a wide variety of applications (e.g. air flow control in fuel cells [3], wind turbine energy capture [4], ABS control, and bioreactors [5]). During this period there have been several innovations that have improved the practicability of ES by increasing convergence speed and eliminating limit cycles. For example, Krstić suggests the addition of dynamic compensators within the ES feedback loop to improve convergence speed [6]. Tan *et al*. analyze various periodic perturbation signals to improve convergence speed [7]. Adetola and Guay, who hypothesize a dynamic plant with no direct measurement of the objective function, guarantee asymptotic convergence using a sufficient richness condition on the reference set-point [8], thus eliminating limit cycles.

This study focuses on asymptotic convergence for the case of a static nonlinear map which is unknown *a priori*. As such, this paper extends the aforementioned research and adds the following two new contributions to the ES control and MPPT bodies of literature. First, we introduce a switching method for ensuring asymptotic convergence to the optimal operating point in extremum seeking control systems, based on Lyapunov stability theory. Secondly, we demonstrate this algorithm in simulation for MPPT problems in PV systems – which itself introduces a novel and control theoretic alternative to traditional MPPT methods.

This paper is organized as follows: Section II describes the extremum seeking control design and our novel Lyapunov-based switching strategy. Section III discusses a case study of the proposed ES method on MPPT for PV systems. Finally, Section IV presents the main conclusions.

II. Extremum Seeking Control

This paper investigates a simple yet widely studied extremum seeking (ES) scheme [1], [5] for static nonlinear maps, shown in Fig. 1, with extensions that guarantee asymptotic convergence. Before embarking on a detailed discussion of this method, we give an intuitive explanation of how extremum seeking works, which can also be found in [1] and [5], but is presented here for completeness. Next we discuss the ES feedback loop design. Finally, we extend the proof presented in [1] to allow the excitation signal to decay exponentially when the system enters a ball around the extremum, using a Lyapunov function. If the optimum value shifts, the Lyapunov function will automatically sense the disturbance and re-enable the sinusoidal perturbation to converge to the new optimal value.

A. An Intuitive Explanation

The control scheme applies a periodic perturbation $a_0\sin(\omega t)$ to the control signal $\hat{u}$, whose signal estimates the

Manuscript received March 15, 2010. This work was supported in part by the National Science Foundation Graduate Research Fellowship Program and National Instruments

S. J. Moura is with the Department of Mechanical Engineering, University of Michigan, Ann Arbor, MI 48109-2133 USA (e-mail: sjmoura@umich.edu).

Y. A. Chang is with the Department of Applications Engineering, National Instruments, Austin, TX 78759 USA (e-mail: andy.chang@ni.com).

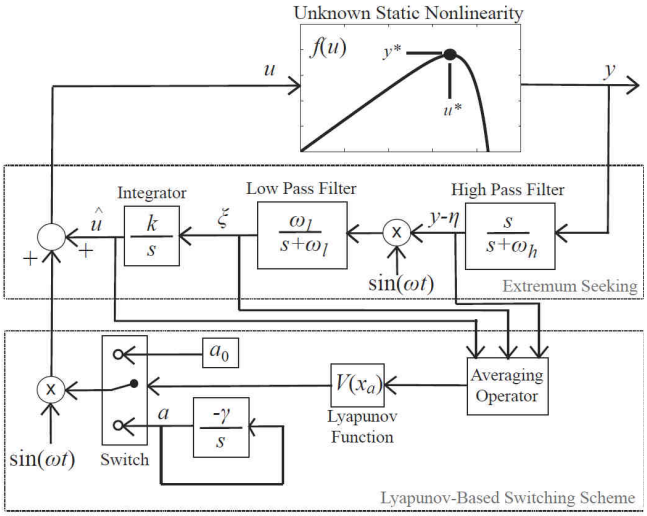

Fig. 1. Block diagram of switched extremum seeking control system.

optimal control input u^*. This control input passes through the unknown static nonlinearity $f(\hat{u} + a_0\sin(\omega t))$, which may be a static approximation of a dynamic plant, to produce a periodic output signal y. The high-pass filter $s/(s+\omega_h)$ then eliminates the DC component of y, and will be in or out of phase with the perturbation signal $a_0\sin(\omega t)$ if $\hat{u}$ is less than or greater than u^*, respectively. This property is important because when the signal $y-\eta$ is multiplied by the perturbation signal $\sin(\omega t)$, the resulting signal has a DC component greater than or less than zero if $\hat{u}$ is less than or greater than u^*, respectively. This DC component is extracted by the low-pass filter $\omega_l/(s+\omega_l)$ and represents the sensitivity $(a_0^2/2)\,\partial f/\partial u\,(\hat{u})$. We may use the gradient update law $\dot{\hat{u}} = k(a_0^2/2)\,\partial f/\partial u\,(\hat{u})$ to force $\hat{u}$ to converge to u^*.

B. ES Control Design

The synthesis process for an extremum seeking controller requires proper selection of the perturbation frequency ω, amplitude a_0, gradient update law gain k, and filter cut-off frequencies ω_h and ω_l. The perturbation frequency must be slower than the slowest plant dynamics to ensure the plant appears as a static nonlinearity from the viewpoint of the ES feedback loop. Mathematically, this can be enforced by ensuring $\omega << \min\{\text{eig}(A)\}$, where A is the state matrix from linearizing the plant. Large values for a_0 and k allow faster convergence rates, but respectively increase oscillation amplitude and sensitivity to disturbances. Therefore, one typically increases these parameter values to obtain maximum convergence speed for a permissible amount of oscillation and sensitivity. The filter cut-off frequencies must be designed in coordination with the perturbation frequency ω. Specifically, the high-pass filter must not attenuate the perturbation frequency, but the low-pass filter should – thus bounding the cut-off frequencies from above. Mathematically $\omega_h < \omega$ and $\omega_l < \omega$. Moreover, the filters should have sufficiently fast dynamics to respond quickly to perturbations in the control input, thereby bounding the cut-off frequencies from below.

Generally, proper selection of the ES parameters is a tuning process [3]. However, the above guidelines are extremely valuable for effective calibration. The ES parameter values used in this report are provided in Table I.

TABLE I
EXTREMUM SEEKING PARAMETERS

Parameter	Description	Value
ω	Perturbation frequeuncy	250 Hz
a_0	Perturbation amplitude	0.015
k	Gradient update law gain	1
ω_h	High-pass filter cut-off freq.	50 Hz
ω_l	Low-pass filter cut-off freq.	50 Hz

C. Averaging Stability Analysis

Extremum seeking using periodic perturbations is particularly appealing because it converges to the local optimum (in the average sense) of a static nonlinearity in real-time, without *a priori* knowledge of the nonlinearity itself. Moreover, ES is self-optimizing in the presence of disturbances that alter the static nonlinearity. However, a general drawback of ES is that once the optimum value is determined, ES causes the system to enter a limit cycle around this value, as opposed to converging to it asymptotically. To eliminate this limit cycle we propose a switching control scheme that effectively decays the amplitude of the periodic perturbation once the system has converged within the interior of a ball about the optimal value. The switch criterion is determined using Lyapunov stability methods. That is, we leverage a Lyapunov function designed from an averaged, linearized model of the original ES feedback system to estimate the proximity to the equilibrium point.[1] Once the Lyapunov function value falls below a threshold, the perturbation decays exponentially. If the Lyapunov function value rises above the threshold, due to an external disturbance for example, the perturbation reengages. Allowing the perturbation to decay exponentially is not new [2], however it is the first application located in a switched scheme, to the authors' knowledge.

We start with the proof proposed by Krstić and Wang [1], which uses averaging theory to approximate the ES system behavior, linearizes it about the optimum, and then shows the resulting Jacobian is Hurwitz. From this proof, our new contribution is to develop a Lyapunov function that senses proximity to the equilibrium point.

The state equations for the closed-loop ES system can be written as follows:

$$\dot{\hat{u}} = k\xi \tag{1}$$

$$\dot{\xi} = -\omega_l\xi - \omega_l\eta\sin(\omega t) + \omega_l f(u)\sin(\omega t) \tag{2}$$

$$\dot{\eta} = -\omega_h\eta + \omega_h f(u) \tag{3}$$

$$u = \hat{u} + a_0\sin(\omega t) \tag{4}$$

[1] The inspiration for this switched controller came from Homework #9 in Professor Jessy Grizzle's EECS 562 Nonlinear Systems and Control course at the University of Michigan, Ann Arbor. In this problem set, we use the same concept to stabilize a pendulum on a cart.

where each equation respectively represents the integrator, low-pass filter, high-pass filter, and perturbed control input.

Now define a new coordinate system that shifts the equilibrium/optimal operating point to the origin

$$\tilde{u} = \hat{u} - u^* \tag{5}$$

$$\tilde{\eta} = \eta - f\left(u^*\right) \tag{6}$$

resulting in the following translated system

$$\dot{\tilde{u}} = k\xi \tag{7}$$

$$\dot{\xi} = -\omega_l \xi - \omega_l \tilde{\eta} \sin\left(\omega t\right) - \omega_l f\left(u^*\right)\sin\left(\omega t\right) + \omega_l f\left(\tilde{u} + u^* + a_0 \sin\left(\omega t\right)\right)\sin\left(\omega t\right) \tag{8}$$

$$\dot{\tilde{\eta}} = -\omega_h \tilde{\eta} - \omega_h f\left(u^*\right) + \omega_h f\left(\tilde{u} + u^* + a_0 \sin \omega t\right) \tag{9}$$

To investigate the stability properties of this system, we consider the averaged system, as done in [1]. This makes intuitive sense because extremum seeking injects a sinusoidal perturbation into the system. Therefore studying the averaged behavior is a appropriate approach. The averaged state variables are defined as follows [9]

$$x_a = \frac{\omega}{2\pi}\int_{t-\frac{2\pi}{\omega}}^{t} x\left(\tau\right)d\tau \tag{11}$$

where the period of the signal is $2\pi/\omega$. Hence, our immediate goal is to use the notion of an average system to investigate the stability properties of the closed loop system. Applying the definition of averaging yields the following system

$$\dot{\tilde{u}}_a = k\xi_a \tag{12}$$

$$\dot{\xi}_a = -\omega_l \xi_a - \omega_l\left(\tilde{\eta}\sin\left(\omega t\right)\right)_a + \omega_l\left(\left(f\left(\tilde{u} + u^* + a_0\sin\left(\omega t\right)\right) - f\left(u^*\right)\right)\sin\left(\omega t\right)\right)_a \tag{13}$$

$$\dot{\tilde{\eta}}_a = -\omega_h \tilde{\eta}_a + \omega_h\left(f\left(\tilde{u} + u^* + a_0\sin\left(\omega t\right)\right) + f\left(u^*\right)\right)_a \tag{14}$$

where $(\cdot)_a$ denotes the averaging operation given by the definition in (11). To simplify this system, the following properties are useful:

- $(\sin(\omega t))_a = 0$
- $(xy)_a \approx x_a\, y_a$. That is, the average of the product of two state variables is approximately equal to the product of the average. This result arises from taking the DC term in a Fourier series expansion [10] – which is appropriate for the present averaging analysis.

These properties imply the second term of (13) is equal to zero, and will help us evaluate the third term of (13) and the second term of (14). Note that these terms are not equal to zero due to the static nonlinearity.

Let us first evaluate the second term of (14), $\omega_h(f(\tilde{u} + u^* + a_0\sin(\omega t)) - f(u^*))_a$. For ease of notation, define

$$h\left(\tilde{u} + a_0\sin\left(\omega t\right)\right) = f\left(\tilde{u} + u^* + a_0\sin\left(\omega t\right)\right) - f\left(u^*\right) \tag{15}$$

The function $h(\tilde{u} + a_0\sin(\omega t))$ translates the extremum of the static nonlinearity to the origin. Let us approximate this function by a quadratic:

$$h\left(\tilde{u} + a_0\sin\left(\omega t\right)\right) \approx b_0 + b_1\left(\tilde{u} + a_0\sin\left(\omega t\right)\right) + b_2\left(\tilde{u} + a_0\sin\left(\omega t\right)\right)^2 \tag{16}$$

Since the origin is located at the optimum, $b_0 = 0$, $b_1 = 0$, and $b_2 < 0$. As we shall see later, the quadratic approximation need only satisfy these conditions to prove the maximum operating point is exponentially stable. That is, we only need to capture the fact that the static nonlinearity is concave and stationary at the maximum operating point (i.e. the first and second order necessary conditions for optimality apply). In other words, a quadratic approximation is sufficient to achieve our immediate goal.

Substituting the quadratic approximation for the translated nonlinear map and applying the averaging definition yields the following nonlinear system

$$\dot{\tilde{u}}_a = k\xi_a \tag{17}$$

$$\dot{\xi}_a = -\omega_l \xi_a + \omega_l\left(\frac{1}{2}b_1 a_0 + b_2 a_0 \tilde{u}\right) \tag{18}$$

$$\dot{\tilde{\eta}}_a = -\omega_h \tilde{\eta}_a + \omega_h\left(b_0 + b_1\tilde{u}_a + b_2\tilde{u}_a^2 + \frac{1}{2}b_2 a_0^2\right) \tag{19}$$

The Jacobian of this system evaluated at the origin is:

$$J = \begin{bmatrix} 0 & k & 0 \\ \omega_l b_2 a_0 & -\omega_l & 0 \\ \omega_h b_1 & 0 & -\omega_h \end{bmatrix} \tag{20}$$

The Jacobian is Hurwitz precisely when $b_2 < 0$, which is true if and only if the static nonlinearity is concave. In the case of estimating the minimum of a convex static map, pick $k < 0$ and $b_2 > 0$, and the resulting Jacobian is Hurwitz. In other words, the extremum seeking approach converges exponentially to both local maxima and minima.

Since the Jacobian is Hurwitz, the averaged system is exponentially stable according to Theorem 4.7 of Khalil [9]. This also satisfies the conditions of Theorem 10.4 of Khalil [9], which states that the original system has a unique exponentially stable periodic orbit about the optimal point. Therefore the ES control system is stable in the sense that the averaged system converges exponentially to the extremum. We leverage this fact to design the Lyapunov-based switching criterion, described next.

D. Lyapunov-Based Switching Scheme

The linearization of the average system about the extremum produces a Jacobian that approximates the system

dynamics near the equilibrium. We now use this Jacobian to develop a quadratic Lyapunov function for the switching control, by solving the following Lyapunov equation for P

$$PJ + J^T P = -Q \tag{21}$$

where Q is taken to be a symmetric matrix (e.g. identity). This results in the following quadratic Lyapunov function

$$V(x_a) = \frac{1}{2} x_a^T P x_a \quad \text{where} \quad x_a = \begin{bmatrix} \tilde{u}_a & \xi_a & \tilde{\eta}_a \end{bmatrix}^T \tag{22}$$

which we use for the following switched control law:

$$u(t) = \begin{cases} \hat{u} + a_0 \sin(\omega t) & \text{if} \quad V(x_a) > \varepsilon \\ \hat{u} + a \sin(\omega t) & \\ \dfrac{da(t)}{dt} = -\gamma a(t) \quad a(0) = a_0 & \text{otherwise} \end{cases} \tag{23}$$

whose conditions are evaluated only when $\sin(\omega t)$ equals zero to ensure the control signal remains continuous in time. Note the dynamics in the decaying amplitude state are stable because the perturbation amplitude has stable dynamics that are decoupled from the remainder of the system [11].

This quadratic Lyapunov function estimates how closely the averaged system converges to the extremum. That is, $V(x_a) \to 0$ as $x_a \to 0$. Once extremum seeking converges sufficiently close to the optimum, the sinusoidal perturbation decays exponentially to zero and the control input arrives at the optimal value u^*. If external disturbances cause the Lyapunov function value to increase above the threshold value ε, then the original amplitude a_0 is used until the system converges to the new extremum. This switched control approach has the following advantageous properties:

1. The proposed scheme eliminates the limit cycles which characterize traditional ES algorithms with sinusoidal excitation signals. Instead, the system converges exponentially to the extremum. In the case of maximum power point tracking of PV systems, which we study in the following section, the proposed algorithm does not oscillate around the maximum power point – a limitation of some existing methods.
2. The sub-level set $\Omega_c = \{x_a \in R^3 \mid V(x) \leq c\}$ with $\dot{V}(x) \leq 0$ is positively invariant, meaning a solution starting in Ω_c remains in Ω_c for all $t \geq 0$. In other words, the Lyapunov function will be decreasing monotonically in time, therefore eliminating chattering behavior.
3. Under external disturbances the state vector x_a may shift away from the origin and produce an instantaneous increase in the Lyapunov function. This causes the perturbation to reengage, and ES proceeds to find the new extremum. Hence, the proposed switched control scheme is self-optimizing with respect to disturbances. This situation is illustrated in the following case study on PV systems, where disturbances may include shading, solar irradiation, and temperature shifts.

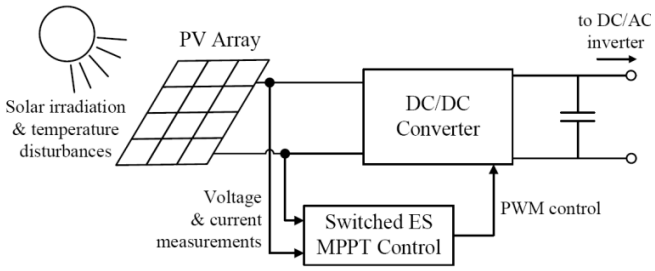

Fig. 2. Photovoltaic (PV) system comprised of a PV array, DC/DC converter, and the proposed switched ES MPPT control algorithm.

TABLE II
PHOTOVOLTAIC ARRAY PARAMETERS

Parameter	Description	Value
A	Ideality factor	1.92
E_{Si}	Band gap energy for silicon	1.11 eV
$I_{0,r}$	Reference reverse saturation current	20×10^{-6} A
$I_{sc,r}$	Reference short-circuit current	2.52 A
k_I	Short-circuit temperature coefficient	0.0017 A/K
k	Boltzmann's constant	1.38×10^{-23} C
n_{cell}	Number of PV cells arranged in series	36
q	Electron charge	1.6×10^{-19} C
R_p	Parallel resistance	9 Ω
R_s	Series resistance	0.0009 Ω
T_r	Reference temperature	301.18 K

Note that to evaluate the Lyapunov function $V(x_a)$, one needs to calculate $\tilde{u}_a$ and therefore know the optimal control input u^*. In this paper we apply an estimate of u^*, which can often be obtained in practice, and demonstrate that Lyap-ES indeed converges to the extremum. For sufficiently inaccurate estimates of u^* the switching condition may never be satisfied and the algorithm degenerates into regular ES, in the worst case. However this can be avoided by appropriate parameter selections for the threshold ε and gain γ [11].

III. CASE STUDY: PHOTOVOLTAIC SYSTEMS

In this section, we investigate the properties and performance of the proposed Lyapunov-based switched extremum seeking scheme on a MPPT problem for PV systems, shown in Fig. 2. Solar energy represents a key opportunity for increasing the role of renewable energy in the electric grid. However, high manufacturing and installation costs have limited the economic viability of PV-based energy production [12]. Therefore, it is vitally important to maximize the energy conversion efficiency of PV arrays. This problem is particularly difficult because high fidelity PV models require detailed semiconductor physics, which are highly dependent on environmental conditions, such as incident solar radiation, temperature, and shading effects. As such, we desire control theoretic techniques that mathematically guarantee asymptotic convergence to the maximum power point (MPP), while

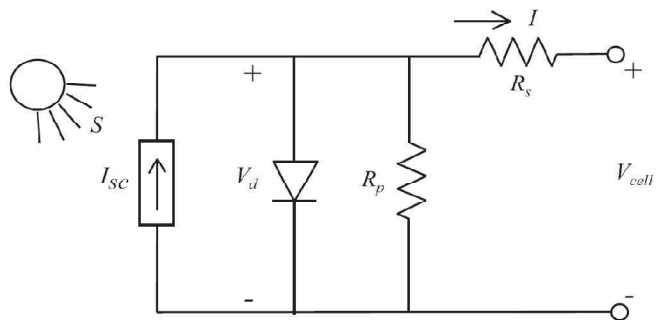

Fig. 3. Equivalent circuit model of PV cell [12], [13].

rejecting disturbances due to changing environments.

First, we summarize a popular equivalent circuit model for PV arrays and a low frequency DC/DC boost converter model. Next we apply Lyap-ES to the PV system and analyze: (1) The asymptotic convergence and self-optimizing behavior under external disturbances due to varying environmental effects, and (2) the algorithm's merits and drawbacks versus traditional ES and MPPT algorithms.

A. PV System Model Development

For the purposes of MPPT we consider an equivalent circuit model [13], [14] of a PV cell shown in Fig. 3. This model consists of an ideal current source I_{sc} in parallel with a diode and resistance R_p, all together in series with resistor R_s, which models contactor and semiconductor material resistance. The ideal current source delivers current in proportion to solar flux S, and is also a function of temperature T. The diode models the effects of the semiconductor material, and also depends on temperature. In total, the PV cell model equations are given by

$$V_d = V_{cell} + IR_s \tag{24}$$

$$I = I_{sc} + I_0\left(e^{\frac{qV_d}{AkT}} - 1\right) - \frac{V_d}{R_p} \tag{25}$$

$$I_{sc} = \left(I_{sc,r} + k_I\left(T - T_r\right)\right)\frac{S}{1000} \tag{26}$$

$$I_0 = I_{0,r}\left(\frac{T}{T_r}\right)^3 \exp\left(\frac{qE_{Si}}{Ak}\right)\left(\frac{1}{T_r} - \frac{1}{T}\right) \tag{27}$$

$$V = n_{cell}V_{cell} \tag{28}$$

The cell model is scaled to represent an array by considering 36 cells in series (28). Since (23)-(27) are implicit nonlinear functions of cell current I and voltage V_{cell}, they must be solved numerically, using Newton's algorithm for example. The parameters for this model are adopted from [13] and provided in Table II.

The PV model is parameterized by environmental conditions - namely incident solar irradiation S and temperature T. Figure 4 demonstrates that current and power increase linearly with incident solar irradiation. Temperature has a more complex impact on current and power. The short circuit current increases slightly with temperature, however the power (and the MPP) decreases as temperature increases. In other words, PV cells operate best in full sunlight and cold temperatures. As a result, we desire a control loop that automatically tracks the MPP under rapidly changing environments to maximize energy conversion efficiency.

A DC/DC boost converter steps up the PV array voltage and provides a control actuator for MPPT, using PWM control on the switches. At the output end of the boost converter a capacitor maintains a roughly constant voltage of 120V and is typically interfaced with the electric grid using a three-phase DC/AC inverter [15]. In this paper, we focus on the boost converter only for the purposes of MPPT, and assume the capacitor maintains a constant 120V at the output. Since the switching frequency is significantly faster than the extremum seeking control loop dynamics, we model the boost converter by the following static relation

$$V = V_{inv}\left(1 - d\right) \tag{29}$$

where V is the PV array voltage, V_{inv} is the constant 120 V capacitor voltage, and d is the duty ratio control input.

B. Simulation Results & Discussion

In this section we demonstrate the proposed switched ES MPPT control approach by (1) analyzing the impact of varying environmental conditions, and (2) comparing it to traditional ES and MPPT methods. In the first part we

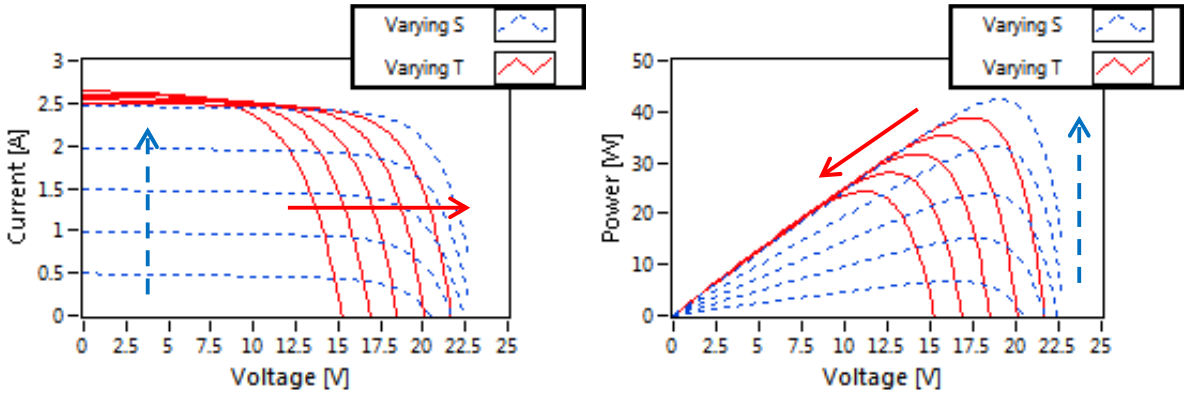

Fig. 4. Characteristic I-V and P-V curves for (a) varying irradiation levels and T = 25ºC, (b) varying temperature levels and S = 1000 W/m^2.

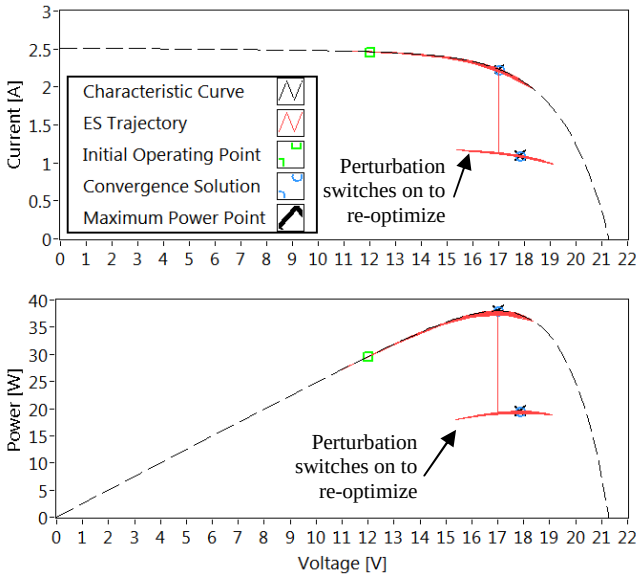

Fig. 5. Trajectories of current and power on PV array characteristic curves for 1000W/m^2 to 500W/m^2 step change in solar irradiation.

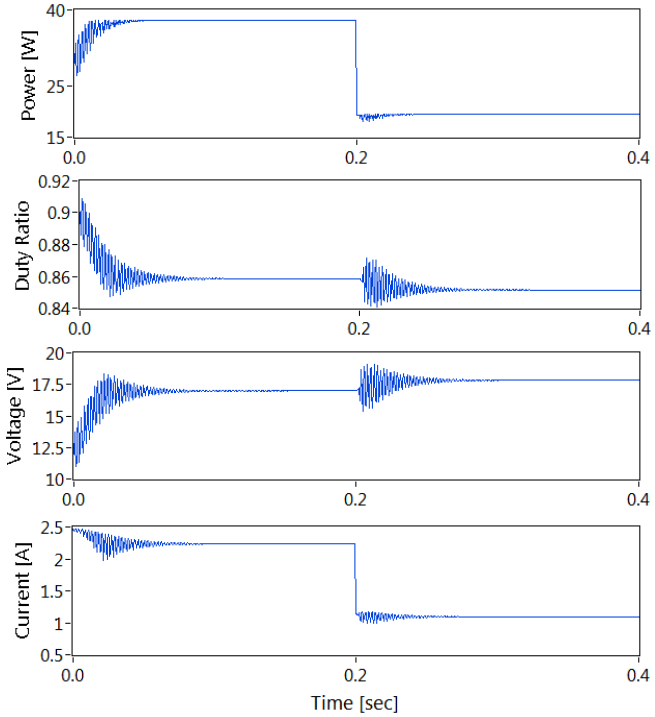

Fig. 6. Time responses of PV array power, duty ratio, voltage, and current for 1000W/m^2 to 500W/m^2 step change in solar irradiation.

impose 1000 W/m^2 of solar irradiation and then provide a 500W/m^2 step change at 200ms. This might model the transient effect of a passing cloud blocking incident sunlight. The duty ratio is initialized at a nominal value of 0.9.

1) Impact of Varying Environmental Conditions

Figure 5 demonstrates the current and power trajectories superimposed on the PV array's characteristic I-V and P-V curves (S = 1000 W/m^2). These plots demonstrate that Lyap-ES indeed achieves the maximum power of 38W at voltage and current values of 17V and 2.24A for S = 1000W/m^2, and maximum power of 19.5W at voltage and current values of 18V and 1.09A for S = 500W/m^2. Moreover, one can see

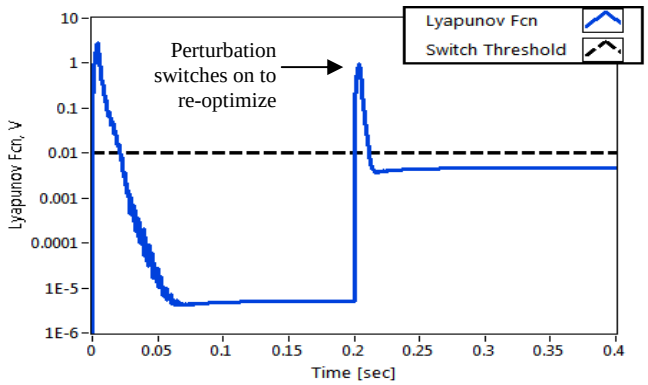

Fig. 7. Lyapunov function and switch threshold for 1000W/m^2 to 500W/m^2 step change in solar irradiation.

how the operating point jumps from the 1000 W/m^2 characteristic curve to the 500 W/m^2 curve during the step change. Immediately after the step change, the operating point is no longer at the MPP. The algorithm senses this change and reengages the perturbation to find the new MPP.

Time responses of power, duty ratio, voltage, and current are provided in Fig. 6. This figure demonstrates how ES injects sinusoidal perturbations into the duty ratio to determine the MPP, which occurs at a duty ratio of 0.8585 for S = 1000W/m^2 and 0.8509 for S = 500W/m^2. Also, the perturbations begin to decay exponentially at 36.5 ms and the duty ratio converges to the optimal value. Once the irradiation changes at 200 ms, the perturbation re-engages to search for the new MPP. Once it converges sufficiently close to the optimal duty ratio, the perturbation amplitude decays exponentially once again.

The switch behavior can be understood by analyzing Fig. 7. At 36.5 ms, the Lyapunov function drops below the switching threshold and hence the perturbation decays. Once the solar flux step change occurs at 200 ms, the averaged states become excited and the Lyapunov function value exceeds the switch threshold. This resets the amplitude of the perturbation to the original value a_0. Then, as the Lyapunov function vanishes below the switch threshold, the perturbation amplitude decays exponentially once again.

2) Comparative Analysis to Existing Methods

This section compares the proposed ES algorithm to standard ES and a traditional MPPT technique: perturb & observe [15], [16]. Although some traditional MPPT methods are somewhat heuristic and may not appeal to the typical control theorist, they often produce satisfactory results and are simple to implement. However they lack guaranteed stability properties and have fundamental limitations. First we review the workhorse MPPT method, perturb & observe. Further interested readers should refer to the review paper [17] and references therein for a more expansive analysis of MPPT techniques.

Perturb & observe algorithms are the most widely used MPPT control systems, where the basic idea is as follows: Periodically perturb the PV array terminal voltage and measure the resulting power output. If the output power increases, then perturb the voltage in the same direction. If power output decreases, then reverse the perturbation. Note

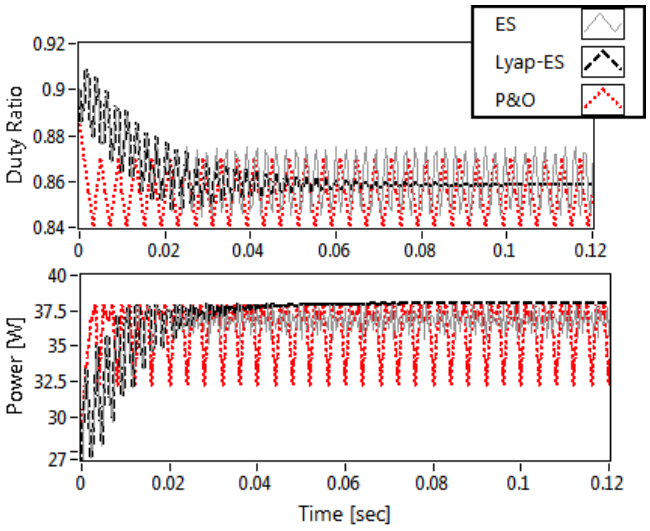

Fig. 8. Comparison of Lyapunov-based switched extremum seeking (Lyap-ES) to basic extremum seeking (ES) and perturb & observe (P&O).

that when the MPP is reached, the P&O algorithm oscillates about this value, thus producing suboptimal energy conversion efficiency. One may reduce the perturbation size to improve efficiency during steady-state, but this reduces convergence speed. Moreover, P&O cannot differentiate if a power increase is due to the voltage perturbation or a disturbance. Therefore, an increase in solar irradiation or drop in temperature will confuse the P&O algorithm.

Figure 8 compares Lyap-ES to two benchmarks: P&O and basic ES (no switching). The scenario under consideration is identical to the previous subsection, however we do not consider varying incident solar irradiation. Moreover, perturbation amplitudes and frequencies of P&O are set to match Lyap-ES, to make the comparison fair.

Several key observations arise from this study. First, ES and Lyap-ES are identical for the first 36.5 ms and then the switch condition is satisfied and Lyap-ES begins to converge to the optimum. Secondly, P&O converges faster than Lyap-ES, for the parameters considered here. Alternative parameter choices for Lyap-ES can close this gap, but sacrifices sensitivity to noise. Finally, ES and P&O oscillate about the MPP whereas Lyap-ES converges to it exactly, thus producing greater power output as shown in the second subplot. This is significant because, for long periods of time, the energy conversion efficiency will be much higher for Lyap-ES than P&O and basic ES.

IV. Conclusion

In this paper we propose a novel Lyapunov-based switched extremum seeking control method (Lyap-ES) that provides a practical extension to existing research on ES by eliminating limit cycles. Specifically, this approach guarantees asymptotic convergence to the extremum of a static map by exponentially decaying the perturbation amplitude once the algorithm reaches a neighborhood of the extremum. This neighborhood is approximated via Lyapunov stability analysis arguments that extend the stability proof originally presented in [1]. We apply Lyap-ES to the MPPT problem in a PV system as a case study to analyze performance. The advantage of Lyap-ES over traditional MPPT methods, e.g. P&O, is that the algorithm converges to the MPP asymptotically without entering a limit cycle. Moreover, the method is self-optimizing with respect to disturbances, such as varying solar irradiation and temperature shifts. It is also computationally efficient and simple to implement in practice. Experimental studies are currently underway in collaboration with National Instruments to demonstrate the model simulation, controller design, and real-time implementation capabilities of LabVIEW. Finally, Lyap-ES also offers a systematic method to solve MPPT problems using systems and control theory.

Acknowledgment

The authors thank Prof. Ian Hiskens at the University of Michigan, Ann Arbor for his advice, helpful discussions, and Winter 2009 course “Grid Integration of Alternative Energy Sources,” which served as the inspiration for this paper.

References

[1] M. Krstić and H.-H. Wang, “Stability of extremum seeking feedback for general nonlinear dynamic systems,” *Automatica*, vol. 36, no. 4, pp. 595-601, Apr. 2000.

[2] D. DeHaan and M. Guay, “Extremum-seeking control of state-constrained nonlinear systems,” *Automatica*, vol. 41, no. 9, pp. 1567-1574, 2005.

[3] Y. A. Chang and S. J. Moura, “Air Flow Control in Fuel Cell Systems: An Extremum Seeking Approach,” *2009 American Control Conference*, 2009, St. Louis, MO, USA.

[4] J. Creaby, Y. Li, and S. Seem, “Maximizing Wind Energy Capture via Extremum Seeking Control,” *2008 ASME Dynamic Systems and Control Conference*, 2008, Ann Arbor, MI, USA.

[5] K. Ariyur and M. Krstić, *Real-time optimization by extremum-seeking control*. Wiley-Interscience, 2003.

[6] M. Krstić, “Performance improvement and limitations in extremum seeking control,” *Systems and Control Letters*, pp. 313-326, 2000.

[7] Y. Tan, D. Nesic, and I. Mareels, “On the choice of dither in extremum seeking systems: A case study,” *Automatica*, vol. 44, no. 5, pp. 1446-1450, 2008.

[8] V. Adetola and M. Guay, “Paramter convergence in adaptive extremum-seeking control,” *Automatic*, vol. 43, no. 1, pp. 105-110, 2007.

[9] H. K. Khalil, Nonlinear systems. Prentice Hall Upper Saddle River, NJ, 2002.

[10] V. A. Caliskan, O. C. Verghese, and A. M. Stankovic, “Multifrequency averaging of DC/DC converters,” *IEEE Transactions on Power Electronics*, vol. 14, no. 1, pp. 124-133, 1999.

[11] S. J. Moura and Y. A. Chang, “Lyapunov-based Switched Extremum Seeking for Maximum Power Point Tracking in Photovoltaic Systems Part 1: Models and Theory,” *in progress*.

[12] “Renewable Energy Cost Trends,” National Renewable Energy Laboratory, Tech. Rep., 2005. [Online]. Available: http://www.nrel.gov/analysis/docs/cost_curves_2005.ppt

[13] G. Vachtsevanos and K. Kalaitzakis, “A Hybrid Photovoltaic Simulator for Utility Interactive Studies,” *IEEE Transactions on Energy Conversion*, vol. EC-2, no. 2, pp. 227-231, 1987.

[14] G. Masters, *Renewable and efficient electric power systems*. John Wiley & Sons, 2004.

[15] J.-M. Kwon, B.-H. Kwon, and K.-H. Nam, “Three-phase photovoltaic system with three-level boosting MPPT control,” *IEEE Transactions on Power Electronics*, vol. 23, no. 5, pp. 2319-2327, 2008.

[16] N. Femia, G. Petrone, G. Spagnuolo, and M. Vitelli, “Optimization of perturb and observe maximum power point tracking method,” *IEEE Trans. on Power Electronics*, vol. 20, no. 4, pp. 963-973, Jul. 2005.

[17] T. Esram and P. L. Chapman, “Comparison of photovoltaic array maximum power point tracking techniques,” *IEEE Transactions on Energy Conversion*, vol. 22, no. 2, pp. 439-449, June 2007.